

# Role of Tet proteins in 5mC to 5hmC conversion, ES-cell self-renewal and inner cell mass specification

Shinsuke Ito<sup>1,2</sup>, Ana C. D'Alessio<sup>1,2</sup>, Olena V. Taranova<sup>1,2</sup>, Kwonho Hong<sup>1,2</sup>, Lawrence C. Sowers<sup>3</sup> & Yi Zhang<sup>1,2</sup>

DNA methylation is one of the best-characterized epigenetic modifications<sup>1–4</sup>. Although the enzymes that catalyse DNA methylation have been characterized, enzymes responsible for demethylation have been elusive<sup>5</sup>. A recent study indicates that the human TET1 protein could catalyse the conversion of 5-methylcytosine (5mC) of DNA to 5-hydroxymethylcytosine (5hmC), raising the possibility that DNA demethylation may be a Tet1-mediated process<sup>6</sup>. Here we extend this study by demonstrating that all three mouse Tet proteins (Tet1, Tet2 and Tet3) can also catalyse a similar reaction. Tet1 has an important role in mouse embryonic stem (ES) cell maintenance through maintaining the expression of Nanog in ES cells. Downregulation of Nanog via Tet1 knockdown correlates with methylation of the *Nanog* promoter, supporting a role for Tet1 in regulating DNA methylation status. Furthermore, knockdown of Tet1 in pre-implantation embryos results in a bias towards trophoblast differentiation. Thus, our studies not only uncover the enzymatic activity of the Tet proteins, but also demonstrate a role for Tet1 in ES cell maintenance and inner cell mass specification.

The Tet protein family includes three members (Tet1, Tet2 and Tet3; Supplementary Fig. 1a). In addition to the dioxygenase motif involved in Fe(II) and  $\alpha$ -ketoglutarate ( $\alpha$ -KG) binding, they also share a conserved cysteine-rich region (Supplementary Fig. 1a, indicated by D and C, respectively). Recent demonstration that human TET1 can convert 5mC to 5hmC in an Fe(II)- and  $\alpha$ -KG-dependent manner<sup>6</sup> prompted us to evaluate whether mouse Tet1 and its homologues possess a similar enzymatic activity. Results shown in Supplementary Fig. 2 demonstrate that overexpression of both mouse Tet1 and Tet2 catalytic domains greatly reduced 5mC staining in both U2OS and HEK293T cells. In contrast, overexpression of mouse Tet3 catalytic domain in these cells had no apparent effect on 5mC staining. The reduced 5mC staining is not due to blocked access of the antibody by the overexpressed proteins, as overexpression of a mutant Tet1 or Tet2 does not affect 5mC staining (Supplementary Fig. 2a). These results indicate that the enzymatic activity of Tet1 is conserved from human to mouse and that both mouse Tet1 and Tet2 can reduce global 5mC levels when overexpressed in a manner that requires the presence of an intact Fe(II) binding site.

Because human TET1 is capable of converting 5mC to 5hmC *in vitro*<sup>6</sup>, we asked whether decreased 5mC staining in cells overexpressing Tet proteins is concomitant with the generation of 5hmC. To this end, we characterized a commercial 5hmC antibody by dot blot and demonstrated that the antibody is 5hmC specific (Supplementary Fig. 3a–c). Competition assays further demonstrated its specificity in immunostaining (Supplementary Fig. 3d). As expected, enforced expression of wild-type Tet1 and Tet2, but not their catalytic mutants, resulted in the generation of 5hmC (Fig. 1a), indicating that Tet proteins can convert 5mC to 5hmC *in vivo* (also see

Supplementary Fig. 3b). Interestingly, whereas the enforced expression of Tet3 does not cause an obvious decrease in 5mC staining (Supplementary Fig. 2), it does result in the generation of 5hmC (Fig. 1a), indicating that Tet3 is indeed enzymatically active *in vivo*.

To evaluate the enzymatic activity *in vitro*, we purified Flag-tagged Tet catalytic domains as well as their corresponding catalytic mutants

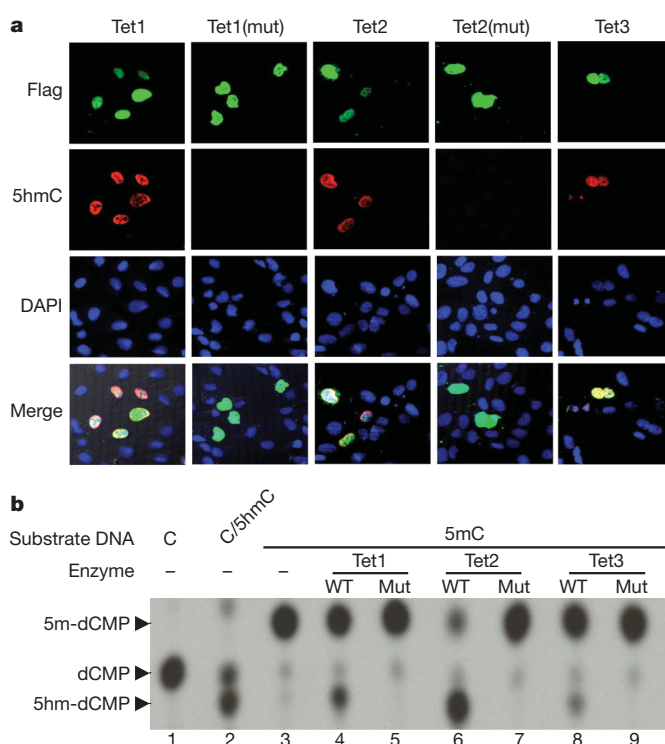


**Figure 1 | The Tet protein family converts 5mC of DNA to 5hmC.**

**a**, Expression of wild-type Tet proteins, but not Fe(II)-binding mutants of Tet1 or Tet2, in U2OS cells results in the generation of 5hmC. Forty-eight hours after transfection, the cells were co-stained with Flag and 5hmC antibodies. Nuclei are counterstained by DAPI. **b**, Recombinant catalytic domains of Tet proteins, but not their catalytic mutants, convert 5mC in DNA oligonucleotides to 5hmC *in vitro*. Double-stranded DNA oligonucleotides containing a fully methylated MspI site were incubated with wild-type and catalytic mutant forms of Flag-Tet1(1367–2039), Flag-Tet2(916–1921), or Flag-Tet3(697–1668) proteins (1:10 enzyme to substrate ratio) in the presence of Fe(II) and  $\alpha$ -KG. Recovered oligonucleotides were digested with MspI, end labelled with T4 DNA kinase, digested with DNaseI and phosphodiesterase, and analysed by TLC. Unmethylated or 5hmC oligonucleotides containing the same sequences were used as a control for marking the migration of dCMP and hmC on TLC plates.

<sup>1</sup>Howard Hughes Medical Institute, <sup>2</sup>Department of Biochemistry and Biophysics, Lineberger Comprehensive Cancer Center, University of North Carolina at Chapel Hill, Chapel Hill, North Carolina 27599-7295, USA. <sup>3</sup>Department of Basic Sciences, Loma Linda University School of Medicine, Loma Linda, California 92350, USA.

from baculovirus-infected SF9 cells (Supplementary Fig. 4a). Incubation of the purified proteins with methylated DNA substrates followed by restriction digestion, end labelling and thin layer chromatography (TLC) assays (Supplementary Fig. 4b, c)<sup>7</sup> demonstrated that wild-type recombinant Tet proteins, but not their corresponding catalytic mutants, were able to generate a radioactive product that co-migrated with 5hmC on TLC plates (compare lanes 4, 6 and 8 with lanes 5, 7 and 9). Given that enforced expression of Tet proteins resulted in the generation of 5hmC (Fig. 1a), we conclude that all of the mouse Tet proteins have the capacity to convert 5mC to 5hmC.

To understand the biological function of the Tet proteins, we examined their expression patterns in various mouse tissues and cell types by real-time quantitative PCR (RT-qPCR). Results shown in Supplementary Fig. 5 revealed that both Tet1 and Tet2, but not Tet3, are expressed in ES cells. This unique expression pattern prompted us to ask whether Tet1 or Tet2 possesses an important function in ES cells. Thus, we generated two independent lentiviral knockdown short hairpin RNAs (shRNAs) for each of the Tet proteins and verified the knockdown efficiency by RT-qPCR (Supplementary Fig. 6a). Notably, knockdown of Tet1, but not Tet2 or Tet3, resulted in morphological abnormality as well as decreased alkaline phosphatase activity (Supplementary Fig. 6b).

In addition to morphological changes, knockdown of Tet1 also resulted in a reduced ES cell growth rate (Fig. 2a), which is not due to a significant increase in apoptosis (Supplementary Fig. 7), but rather to a self-renewal defect (Fig. 2b). To gain an insight into the molecular mechanism underlying the self-renewal defect, we analysed the effects of Tet1 knockdown on the expression of key stem cell factors. Tet1 knockdown reduced Nanog expression (Fig. 2c), which was confirmed by western blotting (Fig. 2d) and immunostaining (Supplementary Fig. 8a). A minor decrease in the levels of Oct4 and Sox2

was also detected (Fig. 2c, d). Consistent with a role for Tet1 in ES cell maintenance, Tet1 messenger RNA and protein are greatly down-regulated upon leukaemia inhibitory factor (LIF) withdrawal or retinoic-acid-induced differentiation (Supplementary Fig. 8b, c). Collectively, the above results indicate that Tet1 has an important role in ES cell self-renewal and maintenance.

To determine whether Tet1 knockdown causes spontaneous differentiation, we stained the cells with the mouse ES cell surface marker SSEA-1 and found that Tet1 knockdown resulted in a 10–15% increase in SSEA-1 negative cells (Supplementary Fig. 9a). RT-qPCR analysis of several markers of early differentiation demonstrates that knockdown of Tet1 in ES cells resulted in selective upregulation of *Cdx2*, *Hand1*, *Gata6* and *Gata4* (Fig. 2e), which is further supported by positive staining of *Cdx2* and Troma-1 (trophoblast markers), and *Gata6* (primitive endoderm marker) in some of the knockdown cells (Supplementary Fig. 9b). Collectively, our data support a role for Tet1 in ES cell maintenance.

To understand the molecular mechanism underlying the function of Tet1 in ES cell maintenance, we investigated whether Nanog is a direct Tet1 target by performing chromatin immunoprecipitation (ChIP) assays using a Tet1 antibody. ChIP-qPCR analysis indicates that Tet1 binds to the proximal and distal tissue-dependent and differentially methylated region (T-DMR) (amplicons 3 and 4) of the *Nanog* promoter identified previously<sup>8</sup>, but it does not bind to region I (amplicon 1) (Fig. 3a). Methyl-DNA immunoprecipitation (MeDIP) analysis demonstrates that knockdown of Tet1 resulted in increased DNA methylation in Tet1 binding regions, but has no effect on region I (Fig. 3a), consistent with a role for Tet1 in maintaining the *Nanog* promoter at a hypomethylated state. Notably, we also observed decreased Sox2 binding in response to Tet1 knockdown (Supplementary Fig. 10). The ability of Tet1 to convert 5mC to 5hmC prompted us to ask whether 5hmC exists in the *Nanog* promoter. Unfortunately the available 5hmC antibody failed to specifically immunoprecipitate 5hmC under our assay conditions (Supplementary Fig. 3e).

Previous studies have demonstrated that the proximal T-DMR of the *Nanog* promoter is demethylated in ES cells, and its methylation correlates with Nanog silencing in trophoblast stem (TS) cells<sup>8</sup>. To verify the MeDIP result, we performed bisulphite sequencing of this transcriptionally relevant region. Results shown in Fig. 3b demonstrate that knockdown of Tet1 resulted in an increase, from 2.8% to 32%, in the levels of DNA methylation at this region. To determine whether increased DNA methylation in Tet1 knockdown cells is responsible for Nanog downregulation, we performed Tet1 knockdown in normal mouse J1 ES cells and in J1 ES cells lacking DNMT1, DNMT3a and DNMT3b (*Dnmt1*<sup>-/-</sup> *Dnmt3a*<sup>-/-</sup> *Dnmt3b*<sup>-/-</sup>, referred to hereafter as DNMT triple knockout)<sup>9</sup>. Similar to that observed in E14 mouse ES cells (Fig. 2c, d), knockdown of Tet1 in mouse J1 ES cells also resulted in downregulation of Nanog expression at both the RNA and protein level (Fig. 3c and Supplementary Fig. 11). However, a similar result is not observed in the DNMT triple knockout J1 ES cells (Fig. 3c and Supplementary Fig. 11), indicating that Nanog downregulation in Tet1 knockdown cells is dependent on DNA methylation. Alternatively, failure of DNMT triple knockout cells to downregulate Nanog expression can be due to the inability of the DNMT triple knockout cells to differentiate<sup>10</sup>. Collectively, these results support that Nanog is a direct Tet1 target and that Tet1 regulates Nanog expression by preventing the *Nanog* promoter from hypermethylation.

To determine whether Tet1's function in ES cells is mediated through maintaining Nanog expression, we investigated whether the phenotypes exhibited in Tet1 knockdown ES cells can be rescued by exogenous Nanog expression. To this end, we generated lentiviral constructs that express *Tet1* shRNAs with or without simultaneous expression of Nanog (Supplementary Fig. 12a). Transduction of ES cells with the lentiviruses expressing the above constructs followed by puromycin selection allowed for the generation of stable knockdown ES cells with or without exogenous Nanog. Both the morphological

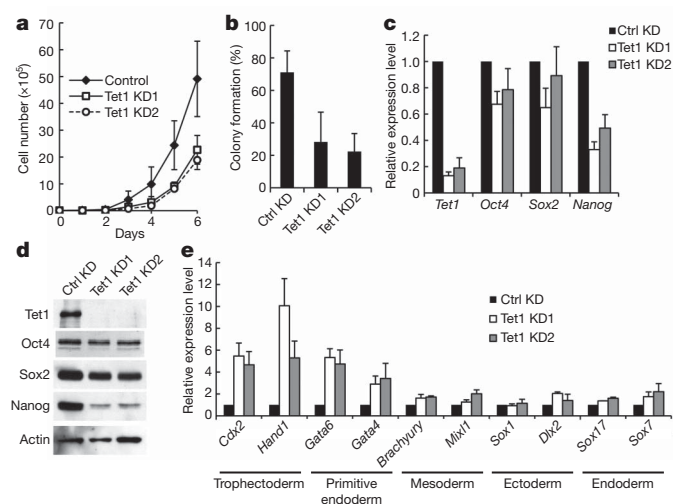


**Figure 2 | Knockdown of Tet1, but not Tet2 or Tet3, impairs ES cell self-renewal and maintenance.** **a**, Tet1 knockdown impairs ES cell proliferation. Growth curves were determined for control and Tet1 knockdown (KD1 and KD2) cells by counting the cell numbers every day. The average cell numbers, with s.d. from three independent experiments, are shown. **b**, Tet1 knockdown impairs ES cell self-renewal. A single control or knockdown cell was plated in each well and its ability to form colonies was evaluated at day 6 after plating. There is no obvious difference between the colony size, but the colony number is greatly reduced in Tet1 knockdown cells when compared to that from control cells. Error bars represent s.d. of three independent experiments. **c**, RT-qPCR analysis of expression levels of *Tet1* and selected stem cell factors in control and knockdown cells. The expression levels in control cells are set as 1. Error bars represent s.d. of three independent experiments. **d**, Western blot analysis of Tet1 and selected stem cell factors in control and knockdown cells. Actin is used as a loading control. **e**, RT-qPCR analysis of the expression of various cell lineage marker genes in control and Tet1 knockdown ES cells. The expression level in control knockdown cells is set as 1. Error bars represent s.d. of three independent experiments.

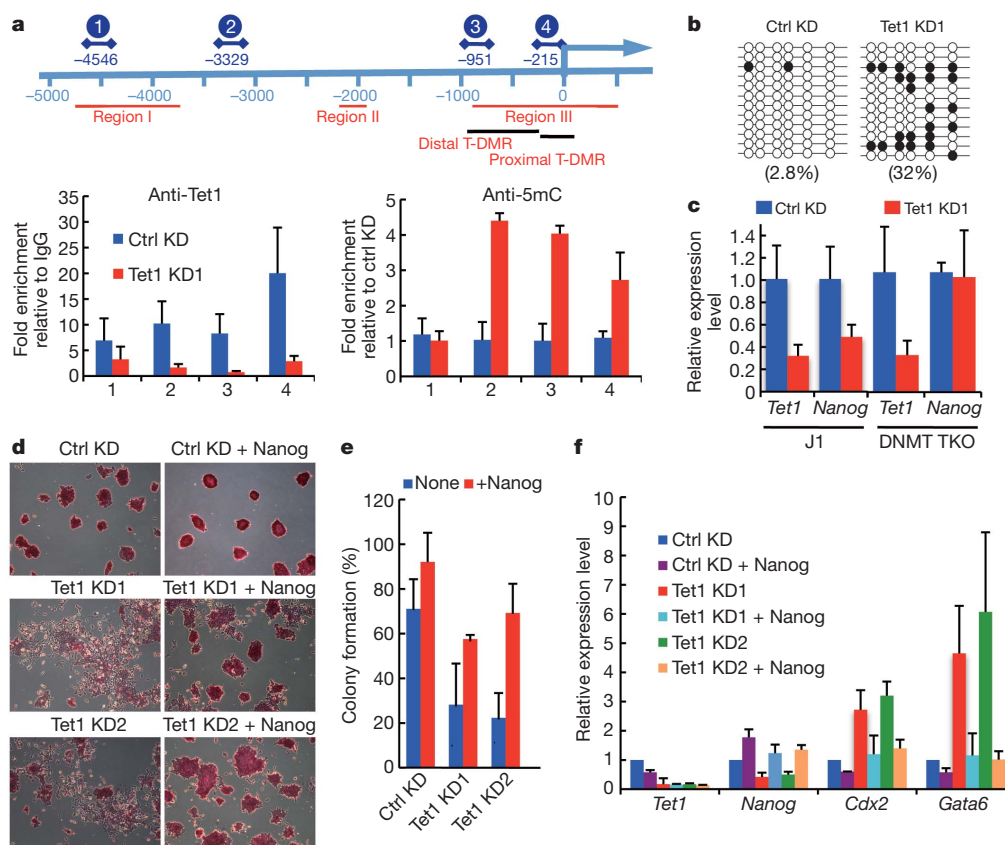


**Figure 3 | Nanog is a direct Tet1 target and Tet1 knockdown phenotypes can be partially rescued by expression of exogenous Nanog.** **a**, ChIP analysis demonstrates that Nanog is a direct target of Tet1. The top panel is a diagram of the *Nanog* gene with the four amplicons indicated. The proximal and distal T-DMR as well as regions I and II are defined as in ref. 8. The numbers in the diagram refer to the gene coordinates. The bottom left panel shows Tet1 enrichment in control and Tet1 knockdown cells relative to IgG controls. The bottom right panel is 5mC enrichment in Tet1 knockdown relative to control knockdown. Results presented are the average of three independent experiments with s.d. **b**, Bisulphite sequencing results indicate that Tet1 knockdown in ES cells results in an increase in DNA methylation at the proximal T-DMR (Fig. 3a) of the *Nanog* promoter. Open circles indicate unmethylated CpG dinucleotides; filled circles indicate methylated CpGs.

changes and the alkaline phosphatase activity of the two independent Tet1 knockdowns are largely rescued by expression of exogenous Nanog (Fig. 3d). In addition, the growth and self-renewal defects caused by Tet1 knockdown are also partially rescued (Fig. 3e and Supplementary Fig. 12b). Consistent with the phenotypic rescue, expression of exogenous Nanog also suppressed upregulation of differentiation genes, such as *Cdx2* and *Gata6*, caused by Tet1 knockdown (Fig. 3f). Collectively, these results support the proposal that *Nanog* is a key target gene that mediates the function of Tet1 in ES cells.

The fact that knockdown of Tet1 results in increased expression of trophoblast and primitive endoderm marker genes raises the possibility that Tet1 may have an important role in the specification of cells of the inner cell mass (ICM). To address this possibility, we examined the expression and cellular localization of Tet1 in pre-implantation embryos by immunostaining. We found that Tet1 is present from the one-cell embryo to the blastocyst stage, and is mainly located in the nuclei. Interestingly, Tet1 is relatively enriched in the ICM compared to trophoblast at the blastocyst stage (Fig. 4a). Consistently, RT-qPCR analysis indicates that the *Tet1* mRNA level is fivefold more in ICM-derived ES cells than in trophoblast stem cells (Fig. 4b). These results indicate that Tet1 might be important for the specification of ICM cells. To address this possibility, short interfering RNAs (siRNAs) that target *Tet1* were injected into

single blastomeres at the two-cell stage and their effect on trophoblast and ICM cell specification was evaluated. To mark the cells derived from the injected blastomere, mRNAs encoding the red fluorescent protein fused to histone H2B (H2B-mRFP) were co-injected with *Tet1* siRNAs. To identify cells of the trophoblast lineage, immunostaining of the key trophoblast transcription factor Cdx2 was performed. An analysis of the distribution of the H2B-mRFP (red) expressing cells that are Cdx2 positive (green) demonstrated that Tet1 knockdown cells preferentially contributed to the trophoblast compared with the ICM cell lineage (Fig. 4c and Supplementary Fig. 13a). Quantification analysis indicated that the ratio of Cdx2-RFP double-positive cells over the total number of RFP-positive cells was significantly increased in Tet1 knockdown when compared with control injections (Fig. 4d), indicating that Tet1 knockdown favours embryonic cell specification towards the trophoblast lineage. Similarly, staining of the Oct4-positive ICM cells indicated that Tet1 knockdown prevents embryonic cell specification towards the ICM (Fig. 4e, f and Supplementary Fig. 13b). Collectively, these studies support a role for Tet1 in the formation of ICM consistent with the studies performed in ES cells.

Whether DNA methylation is a reversible reaction and, if so, what the underlying mechanism is has been a subject of debate<sup>5</sup>. Although there is substantial evidence indicating genome-wide<sup>11,12</sup> as well as



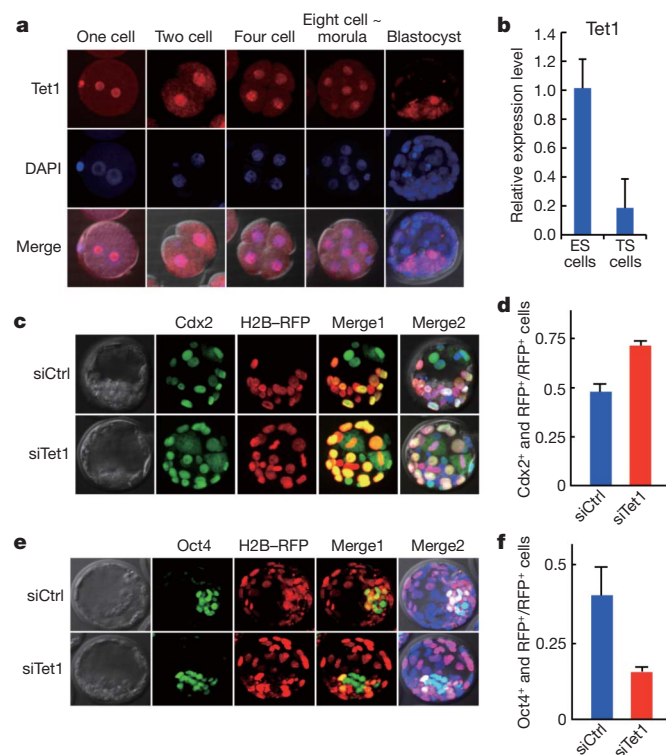


**Figure 4 | Tet1 is required for ICM cell specification in blastocysts.** **a**, Tet1 protein is present in the nuclei of pre-implantation mouse embryos. Mouse embryos at different developmental stages (one-cell to blastocyst) were stained with Tet1 antibody. Note that Tet1 is relatively enriched in the ICM when compared to that in the trophectodermal cells at the blastocyst stage. **b**, RT-qPCR demonstrates that ICM-derived ES cells expressed higher levels of Tet1 when compared with trophoblast stem cells (TS cells). Error bars represent s.d. of three independent experiments. **c**, Knockdown of Tet1 at the two-cell stage promotes trophectoderm cell specification. Representative Z-stack image of a control and a knockdown blastocyst are shown. Trophectoderm lineage cells are Cdx2 positive (green). Control knockdown and Tet1 knockdown cells are marked in red. Cells with yellow colour in the merge panels are trophectoderm lineage cells that were derived from the injected blastomere. **d**, Ratio of Cdx2<sup>+</sup>RFP<sup>+</sup> cells over RFP<sup>+</sup> cells from control knockdown and Tet1 knockdown. Eight control-injected embryos and nine *Tet1* siRNA injected embryos were used for the quantification analysis ( $P < 0.001$ ). Error bars represent s.e.m. **e**, Knockdown of Tet1 prevents cells from contributing to the ICM. Representative Z-stack images with Oct4 staining (green) in control and Tet1 knockdown cells (red). Cells with yellow colour in the merge panels are the cells derived from the injected blastomere that contributed to the ICM. **f**, Ratio of Oct4<sup>+</sup>RFP<sup>+</sup> cells over RFP<sup>+</sup> cells from control knockdown and Tet1 knockdown. Seven control-injected embryos and seven *Tet1* siRNA injected embryos were used for the quantification analysis ( $P = 0.004$ ). Error bars represent s.e.m.

locus-specific DNA demethylation<sup>13</sup>, the molecules that mediate DNA demethylation have been elusive<sup>5</sup>. Interestingly, a recent study indicated that the cytidine deaminase AID is involved in DNA demethylation in mouse primordial germ cells<sup>14</sup>, although significant DNA demethylation still occurs in primordial germ cells in the absence of AID. Using live cell imaging coupled with siRNA knockdown in mouse zygotes, we have recently demonstrated that the transcriptional elongator is required for paternal genome demethylation in zygotes<sup>15</sup>. However, how the elongator participates in the demethylation process is unknown. In search of an enzyme that can modulate DNA methylation, a recent study revealed that human Tet1 could convert 5mC of DNA to 5hmC<sup>6</sup>. Here we confirm and extend this study by demonstrating that all three mouse Tet proteins have similar enzymatic activities. Whether 5hmC can be further processed to C by an enzyme-catalysed process or by base excision remains to be determined. In this regard, we note that a 5hmC-specific DNA glycosylase activity has been previously reported<sup>16</sup>.

In addition to demonstrating the enzymatic activity of the Tet proteins, we provide evidence indicating that Tet1 is a novel factor of the ES cell self-renewal network. Our data support a working model by which Tet1 and DNMTs coordinately regulate Nanog expression. In ES cells, high levels of Tet1 either block the access of DNMTs or result in the enzymatic conversion of 5mC to 5hmC, which is further processed by another enzyme (directly or indirectly through a repair-based mechanism) to C, for maintained Nanog expression. On the other hand, when Tet1 is downregulated in ES cells, DNMTs methylate the *Nanog* promoter, leading to the down-regulation of Nanog expression and consequent loss of ES cell identity. Previous studies have demonstrated a role for Nanog in ES cell self-renewal<sup>17,18</sup>. Furthermore, Tet1 also seems to have a role in maintaining ES cell fate, which is consistent with its role in ICM cell specification. Future studies should reveal the precise mechanism underlying Tet1's function in these processes.

## METHODS SUMMARY

**Mouse ES cell culture, Tet knockdown and Nanog rescue.** Mouse E14Tg2A ES cells were maintained on gelatin-coated dishes in Glasgow Minimum Essential medium (GMEM; GIBCO), supplemented with 15% heat-inactivated fetal bovine serum, 55  $\mu$ M  $\beta$ -mercaptoethanol (GIBCO), 2 mM L-glutamine, 0.1 mM MEM non-essential amino acid, 5,000 units ml<sup>-1</sup> penicillin/streptomycin and 1,000 units ml<sup>-1</sup> of ESGRO (Chemicon) under feeder-free conditions. To knockdown Tet proteins, lentiviral transduction was performed as described previously<sup>19</sup>. Short-hairpin RNA (shRNA) sequences (Supplementary Table 2) were cloned into pTY vector under the control of the U6 promoter. To rescue Tet1 knockdown with Nanog, complementary DNA of *Nanog* was placed downstream of the puromycin-resistant gene and foot-and-mouth disease virus 2A segment (Supplementary Fig. 12a).

**Knockdown of Tet1 in two-cell embryos, embryo staining and confocal images.** For Tet1 knockdown in two-cell embryos, siRNAs (KD1 and KD2 mix, 2  $\mu$ M each) that target Tet1 or siControl were co-injected into one of the blastomeres with H2B-mRFP (mRFP, 50 ng  $\mu$ l<sup>-1</sup>). The injected embryos were cultured in KSOM media (EmbryoMax, Millipore) to the blastocyst stage. Embryos at various developmental stages were incubated in blocking solution containing anti-Tet1, anti-Cdx2, or anti-Oct4 antibody for 1 h at room temperature. After washing with PBS, cells were incubated in FITC or Rhodamine-conjugated secondary antibody for 1 h at room temperature and were counterstained with 4',6-diamidino-2-phenylindole (DAPI). Fluorescent images were captured using a confocal microscope with a spinning disk (CSU-10, Yokogawa) and an EM-CCD camera (ImagEM, Hamamatsu). All images were acquired as 2  $\mu$ m Z-axis intervals and reconstituted using Axiovision (Zeiss).

**Full Methods** and any associated references are available in the online version of the paper at [www.nature.com/nature](http://www.nature.com/nature).

Received 15 March; accepted 28 June 2010.

Published online 18 July; corrected 26 August 2010 (see full-text HTML version for details).

- Bird, A. DNA methylation patterns and epigenetic memory. *Genes Dev.* 16, 6–21 (2002).
- Cedar, H. & Bergman, Y. Linking DNA methylation and histone modification: patterns and paradigms. *Nature Rev. Genet.* 10, 295–304 (2009).
- Sasaki, H. & Matsui, Y. Epigenetic events in mammalian germ-cell development: reprogramming and beyond. *Nature Rev. Genet.* 2008, 129–140 (2008).
- Surani, M. A., Hayashi, K. & Hajkova, P. Genetic and epigenetic regulators of pluripotency. *Cell* 128, 747–762 (2007).
- Ooi, S. K. & Bestor, T. H. The colorful history of active DNA demethylation. *Cell* 133, 1145–1148 (2008).
- Tahiliani, M. et al. Conversion of 5-methylcytosine to 5-hydroxymethylcytosine in mammalian DNA by MLL partner TET1. *Science* 324, 930–935 (2009).
- Tardy-Planechaud, S., Fujimoto, J., Lin, S. S. & Sowers, L. C. Solid phase synthesis and restriction endonuclease cleavage of oligodeoxynucleotides containing 5-(hydroxymethyl)-cytosine. *Nucleic Acids Res.* 25, 553–559 (1997).
- Hattori, N. et al. Epigenetic regulation of *Nanog* gene in embryonic stem and trophoblast stem cells. *Genes Cells* 12, 387–396 (2007).
- Tsumura, A. et al. Maintenance of self-renewal ability of mouse embryonic stem cells in the absence of DNA methyltransferases Dnmt1, Dnmt3a and Dnmt3b. *Genes Cells* 11, 805–814 (2006).
- Jackson, M. et al. Severe global DNA hypomethylation blocks differentiation and induces histone hyperacetylation in embryonic stem cells. *Mol. Cell. Biol.* 24, 8862–8871 (2004).
- Mayer, W., Niveleau, A., Walter, J., Fundele, R. & Haaf, T. Demethylation of the zygotic paternal genome. *Nature* 403, 501–502 (2000).

12. Oswald, J. *et al.* Active demethylation of the paternal genome in the mouse zygote. *Curr. Biol.* **10**, 475–478 (2000).
13. Bruniquel, D. & Schwartz, R. H. Selective, stable demethylation of the interleukin-2 gene enhances transcription by an active process. *Nature Immunol.* **4**, 235–240 (2003).
14. Popp, C. *et al.* Genome-wide erasure of DNA methylation in mouse primordial germ cells is affected by AID deficiency. *Nature* **463**, 1101–1105 (2010).
15. Okada, Y., Yamagata, K., Hong, K., Wakayama, T. & Zhang, Y. A role for the elongator complex in zygotic paternal genome demethylation. *Nature* **463**, 554–558 (2010).
16. Cannon, S. V., Cummings, A. & Teebor, G. W. 5-Hydroxymethylcytosine DNA glycosylase activity in mammalian tissue. *Biochem. Biophys. Res. Commun.* **151**, 1173–1179 (1988).
17. Chambers, I. *et al.* Nanog safeguards pluripotency and mediates germline development. *Nature* **450**, 1230–1234 (2007).
18. Ivanova, N. *et al.* Dissecting self-renewal in stem cells with RNA interference. *Nature* **442**, 533–538 (2006).
19. He, J., Kallin, E. M., Tsukada, Y. & Zhang, Y. The H3K36 demethylase Jhdmlb/Kdm2b regulates cell proliferation and senescence through p15<sup>ink4b</sup>. *Nature Struct. Mol. Biol.* **15**, 1169–1175 (2008).

**Supplementary Information** is linked to the online version of the paper at [www.nature.com/nature](http://www.nature.com/nature).

**Acknowledgements** We thank M. Okano for the J1 and DNMT triple knockout ES cells; J. He and A. Nguyen for help in FACS sorting; and S. Wu for critical reading of the manuscript. This work was supported by NIH grants GM68804 (to Y.Z.) and CA084487 (to L.C.S.). S.I. is a research fellow of the Japan Society for the Promotion of Science. O.T. is a postdoctoral fellow of Juvenile Diabetes Research Foundation International. Y.Z. is an Investigator of the Howard Hughes Medical Institute.

**Author Contributions** Y.Z. conceived the project and wrote the manuscript. S.I., A.C.D., O.V.T. and K.H. designed and performed the experiments. L.C.S. provided the oligonucleotide substrates.

**Author Information** Reprints and permissions information is available at [www.nature.com/reprints](http://www.nature.com/reprints). The authors declare no competing financial interests. Readers are welcome to comment on the online version of this article at [www.nature.com/nature](http://www.nature.com/nature). Correspondence and requests for materials should be addressed to Y.Z. ([yi\\_zhang@med.unc.edu](mailto:yi_zhang@med.unc.edu)).

## METHODS

**Constructs and antibodies.** Mouse *Tet1* (GU079948) and *Tet2* (GU079949) cDNAs were cloned from E14Tg2A ES cells, and mouse *Tet3* (Q8BG87) was cloned from ovaries of CD1 mice. Clones were generated using the MonsterScript 1st strand cDNA synthesis kit (Epicentre) followed by PCR amplification with FailSafe (Epicentre). DNA fragments were subcloned into the Invitrogen TA cloning kit following the manufacturer's protocol and verified by DNA sequencing. Plasmids encoding Flag-tagged catalytic domains of *Tet1* (amino acids 1367–2039), *Tet2*(916–1921) and *Tet3*(697–1668) were generated by subcloning of the DNA fragments into BamHI and XbaI sites (for *Tet1*) or EcoRI site (for *Tet2*, *Tet3*) of an N-terminal Flag-tagged pcDNA3 vector or an N-terminal Flag-tagged pFASTBAC vector. The catalytic mutants encoded by pcDNA3-Flag-*Tet1* (H1652Y, D1654A) and pcDNA3-Flag-*Tet2* (H1304Y, D1306A) were generated using the QuikChange II XL site-directed mutagenesis kit (Stratagene). For mTet1 antibody production, cDNA encoding mTet1(1–184) was cloned into the BamHI and XbaI sites of pProEx HTb. All of the constructs generated through PCR were verified by DNA sequencing.

mTet1 His-tagged antigen (1–184) was expressed in *Escherichia coli* and purified using Talon superflow metal affinity resin (Clontech). Rabbit polyclonal anti-sera against mTet1(1–184) was generated by Pocono Rabbit Farm and Laboratory, Inc. The specificity of the affinity-purified antibodies was tested using extracts from the control and *Tet1* knockdown mES cells. The rabbit 5hmC antibody was purchased from Active Motif (catalogue no. 39769). All of the other antibodies used in this study are listed in Supplementary Table 1.

**Recombinant protein expression, purification and activity assays.** For production of recombinant proteins, the catalytic domains of *Tet1*, *Tet2* and *Tet3* cDNAs were cloned into a modified pFastbac-HTb (Invitrogen) vector containing an N-terminal Flag tag. Generation of baculovirus that expresses Flag-*Tet1*(CD), Flag-*Tet2*(CD), or Flag-*Tet3*(CD) was performed using the Bacto-Bac system (Invitrogen) according to the manufacturer's instructions. The recombinant proteins were purified from infected Sf9 cells with the anti-Flag M2 antibody agarose affinity gel (Sigma-Aldrich) and eluted with buffer containing 10 mM Tris-HCl pH 8.0, 150 mM NaCl, 1 mM DTT, 15% glycerol and 0.2  $\mu\text{g ml}^{-1}$  Flag peptide.

An *in vitro* activity assay was performed using a modified procedure described previously<sup>20</sup>. Briefly, 5  $\mu\text{g}$  of purified proteins were incubated with 0.5  $\mu\text{g}$  of double-stranded oligonucleotide substrates in 50 mM HEPES, pH 8, 75  $\mu\text{M}$   $\text{Fe}(\text{NH}_4)_2(\text{SO}_4)_2$ , 2 mM ascorbate, and 1 mM  $\alpha$ -KG for 3 h at 37 °C. Oligonucleotide substrates were purified using Qiaquick Nucleotide Removal kit (Qiagen) and then digested with MspI. The 5' end of the digested DNA was treated with calf alkaline phosphatase, and labelled with [ $\gamma$ -<sup>32</sup>P]ATP and T4 polynucleotide kinase. Labelled fragments were ethanol-precipitated, and digested with 10  $\mu\text{g}$  of DNase I and 10  $\mu\text{g}$  of phosphodiesterase I in the presence of 15 mM  $\text{MgCl}_2$ , 2 mM  $\text{CaCl}_2$  at 37 °C. One microlitre of digestion products was spotted on a PEI-cellulose TLC plate (Merck) and separated in isobutyric acid:water:ammonium hydroxide (66:20:2) running buffer. After drying, the TLC plate was exposed to X-ray film.

**Mouse ES cell culture, Tet knockdown, RNA isolation and qPCR.** Mouse feeder free E14Tg2A ES cells were maintained on gelatin-coated dishes in Glasgow Minimum Essential medium (GMEM; GIBCO), supplemented with 15% heat-inactivated fetal bovine serum, 55  $\mu\text{M}$   $\beta$ -mercaptoethanol (GIBCO), 2 mM L-glutamine, 0.1 mM MEM non-essential amino acid, 5,000 units  $\text{ml}^{-1}$  penicillin/streptomycin and 1,000 units  $\text{ml}^{-1}$  of ESGRO (Chemicon) under feeder-free conditions. J1 ES cells and *Dnmt1*<sup>-/-</sup>*Dnmt3a*<sup>-/-</sup>*Dnmt3b*<sup>-/-</sup> (DNMT triple knockout) ES cells were maintained on gelatin-coated dishes with mitotically inactivated mouse embryonic fibroblasts. Alkaline phosphatase staining was performed with the Alkaline Phosphatase Detection kit (Chemicon). For growth curve analysis, control and knockdown ES cells were plated at  $1 \times 10^3$  cells  $\text{cm}^{-2}$  and counted for six consecutive days. For self-renewal analysis cells were plated on 96-well plates at single cell density and the number of colonies on each plate was counted six days after plating.

To knockdown Tet proteins, lentiviral transduction was performed in mouse ES cells as described previously<sup>19</sup>. Short-hairpin RNA (shRNA) sequences (Supplementary Table 2) were cloned into the pTY vector under the U6 promoter. To rescue *Tet1* knockdown with Nanog, cDNA of Nanog was placed downstream of the puromycin-resistant gene and foot-and-mouth disease virus 2A segment (Supplementary Fig. 12), which enables multicistronic expression of transgenes in ES cells using a single promoter<sup>21</sup>.

Total RNA from mouse tissues was isolated using Trizol reagent (Invitrogen) and total RNA from cultured cells was isolated using the RNeasy Mini kit (Qiagen), and cDNA was generated with the Improm-ITM Reverse Transcription System (Promega). Real-time quantitative PCR reactions were performed on an ABI PRISM 7700 Sequence Detection System (Applied

Biosystems) using SYBR Green reagent (Invitrogen). cDNA levels of target genes were analysed using comparative  $C_t$  methods, where  $C_t$  is the cycle threshold number, and normalized to GAPDH. RT-qPCR primers are listed in Supplementary Table 3.

**Immunostaining, confocal images, FACS analysis and apoptosis assay.** Mouse ES cells, U2OS cells, or HEK293T cells were plated onto glass coverslips and U2OS cells, or HEK293T cells were transfected with constructs encoding the wild-type or catalytic mutants and cultured for 2 days. Cells were fixed in 4% paraformaldehyde for 15 min. The cells were then washed with cold PBS and permeabilized for 15 min with cold PBS containing 0.4% Triton X-100. Permeabilized cells were then washed and incubated for 1 h with blocking buffer (10% donkey serum, 3% bovine serum albumin in PBS containing 0.1% Triton X-100) before incubation with primary antibodies overnight in a humidified chamber at 4 °C. For 5mC or 5hmC staining, permeabilized cells were denatured with 2 N HCl for 15 min, neutralized with 100 mM Tris-HCl (pH 8.5) for 10 min before blocking. The primary antibodies used are listed in Supplementary Table 1. After three consecutive 5-min washes with PBS, cells were incubated with secondary antibodies and DAPI for 30 min. Cells were washed again three times with PBS and then mounted in fluorescent mounting medium (Dako). Images were acquired using Zeiss immunofluorescence microscope Axiovert 200 and Axiovision software.

For pre-implantation embryo staining, embryos at various developmental stages were incubated in blocking solution containing anti-*Tet1*, anti-*Cdx2*, or anti-Oct4 antibody for 1 h at room temperature. After washing with PBS, cells were incubated in FITC or Rhodamine-conjugated secondary antibody for 1 h at room temperature. Embryos were counterstained with DAPI. Fluorescent images were captured using a confocal microscope with a spinning disk (CSU-10, Yokogawa) and an EM-CCD camera (Imagem, Hamamatsu). All images were acquired as 2  $\mu\text{m}$  Z-axis intervals and reconstituted using Axiovision (Zeiss).

For apoptosis analysis, cells were stained with active caspase and the Annexin V-FITC apoptosis detection kit with propidium iodide (EBiosciences) following the manufacturer's instruction. Fluorescence intensity was determined by flow cytometry on a Becton Dickinson FACScan. Data acquisition and analysis were performed with Summit 4.0 software.

**Knockdown of Tet1 in two-cell embryos.** Five- to six-week-old female BDF1 (C57BL6 X DBA2) hybrid mice were superovulated by injecting 7.5 International Units (I.U.) of PMSG (Harbour, UCLA) and 7.5 I.U. of hCG (Sigma Aldrich). For knockdown at the two-cell stage, siRNAs (KD1 and KD2, 2  $\mu\text{M}$  each) that target *Tet1* or siControl were co-injected into one of the blastomeres with histone H2B fused to monomeric red fluorescent protein (mRFP, 50  $\text{ng } \mu\text{l}^{-1}$ ). The injected embryos were cultured in KSOM media (EmbryoMax, Millipore) to blastocyst stage.

**ChIP assays and bisulphite sequencing.** Cells were fixed with a final concentration of 1% formaldehyde. After incubation at room temperature for 10 min, the reaction was stopped by the addition of 125 mM glycine. Chromatin immunoprecipitation (ChIP) assays were performed using a protocol associated with the ChIP assay kit (Upstate Biotechnology). After extensive washing, ChIPed DNA was eluted from the beads and analysed on an ABI 7300 Real Time PCR System (Applied Biosystems) using SYBR Green reagent (Invitrogen). Primer sequences and antibodies are listed in Supplementary Tables 4 and 1, respectively.

Bisulphite sequencing was performed as described previously with minor modifications<sup>22</sup>. Five micrograms of sodium-bisulphite-treated DNA samples was subjected to PCR amplification using the first set of primers; PCR products were used as templates for a subsequent PCR reaction using nested primers. The PCR products of the second reaction were then subcloned using the Invitrogen TA cloning kit following the manufacturer's instruction. PCRs and subcloning were performed in duplicate for each sample. The clones were sequenced using the M13 reverse primer. Primers for bisulphite sequencing are listed in Supplementary Table 5.

**Dot-blot assay.** Different amounts of standard DNA (949 bp, Zymo Research, catalogue no. D5405) where C is either C, 5mC, or 5hmC, or genomic DNA were denatured with 0.1 N NaOH and spotted on nitrocellulose membranes (BioRad; catalogue no. 162-0112). The membrane was baked at 80 °C and then blocked in 5% skimmed milk in TBS containing 0.1% Tween 20 (TBST) for 1 h at room temperature. The membranes were then incubated with 1:10,000 dilution of 5hmC (Active Motif) or 1:1,000 dilution of 5mC (Eurogentec) overnight at 4 °C. After three rounds of washes with TBST, membranes were incubated with 1:2,000 dilution of HRP-conjugated anti-rabbit or anti-mouse IgG secondary antibody, respectively. The membranes were then washed with TBST and treated with ECL.

**Hydroxymethyl-DNA immunoprecipitation (HmeDIP).** Ten nanograms of control methylated or hydroxymethylated DNA were diluted in 480  $\mu\text{l}$  1 $\times$  TE buffer. DNA was heat-denatured for 10 min at 95 °C, and quickly cooled on ice for 5 min. Then 100  $\mu\text{l}$  of 5 $\times$  IP buffer (50 mM sodium phosphate, pH 7.0;

700 mM NaCl; 0.25% Triton X-100) was added to the denatured DNA. Five microlitres of monoclonal antibody for 5-methylcytosine (Eurogentec), HmeC (active Motif) or rabbit IgG (Santa Cruz) were added, and the DNA–antibody complexes were captured for 2 h with protein G magnetic Dynabeads (Invitrogen) pre-blocked in 0.5% BSA in 1× PBS. Beads were washed three times with 1× IP buffer and re-suspended in 250 µl digestion buffer (50 mM Tris-HCl, pH 8.0; 10 mM EDTA; 0.5% SDS). To elute the DNA, 3.5 µl proteinase K was added and incubated overnight on a rotating platform at 55 °C. After a brief spin, the DNA was extracted with phenol-chloroform followed by ethanol

precipitation and qPCR with primers H/me-1- F (AGGTGGAGGAAGG TGATGTC) and H/me-1- R (ATAAACCGAACCGCTACACC).

20. Chen, Z. J. & Pikaard, C. S. Epigenetic silencing of RNA polymerase I transcription: a role for DNA methylation and histone modification in nucleolar dominance. *Genes Dev.* **11**, 2124–2136 (1997).
21. Hasegawa, K., Cowan, A. B., Nakatsuji, N. & Suemori, H. Efficient multicistronic expression of a transgene in human embryonic stem cells. *Stem Cells* **25**, 1707–1712 (2007).
22. Clark, S. J., Harrison, J., Paul, C. L. & Frommer, M. High sensitivity mapping of methylated cytosines. *Nucleic Acids Res.* **22**, 2990–2997 (1994).